Sensitivity of a Cloud Microphysical Model to an Urban Environment

HARRY T. OCHS III AND RICHARD G. SEMONIN

Illinois State Water Survey, Urbana 61801

(Manuscript received 29 June 1978, in final form 11 May 1979)

ABSTRACT

Observations showed increased concentrations of cloud condensation nuclei (CCN) in air samples collected over and downwind of St. Louis when compared to upwind samples. Aircraft observations of urban clouds showed corresponding increased concentrations of cloud base droplets. In addition, observations indicated higher cloud bases and decreased elevations of average first echo base heights in the St. Louis/East St. Louis area as compared with similar clouds over rural areas.

The purpose of this paper is to examine the possible role of CCN chemical composition and number concentration in producing the observed phenomena. A closed parcel model of condensation and collection was employed for this purpose. The results suggest that the observed differences of depth from cloud base to first echo height between urban and rural clouds do not result from concentration differences in any CCN size range. Results of model calculations also suggest that variations in chemical composition of the largest CCN (>1.0 μm radius) were not responsible for the observed urban/rural differences. A hypothesis based on observations and model results is presented for explaining the observed differences in cloud base to first echo depth in terms of differences between the evolution and strength of updrafts in urban and rural clouds.

1. Introduction

METROMEX field project research results showed the existence of the severe weather anomaly in proximity of St. Louis (Huff and Changnon, 1972) which satisfies one of the project goals (Changnon *et al.*, 1971). In an effort to obtain data that would illuminate the physical processes that contribute to the anomaly, aircraft probed clouds that had ingested urban modified air as well as those unaffected by the St. Louis urban complex. Flights were conducted in storm updraft areas to seek data on microphysical and mesoscale alterations related to urban conditions. These measurements included cloud condensation nuclei (CCN), cloud microphysical structure, and the three-dimensional thermodynamic structure. Fitzgerald and Spyers-Duran (1973) reported observations that indicated a definite alteration toward greater droplet concentrations and more narrow distributions in the urban and downwind fair-weather cumulus as opposed to similar upwind clouds.

These observations led Braham (1974) and Semonin and Changnon (1974) to hypothesize the existence of giant condensation nuclei to justify the observed formation of urban radar first echoes at a lower altitude than rural echoes. The observed droplet spectra in urban and downwind clouds were suggestive of a deterrent to precipitation formation since the coalescence process would be inhibited by a narrow distribution. The radar first echo statistics, however, indicated an enhanced development of precipitation particles below the freezing level. A sophisticated numerical model of cloud microphysics was used to attempt to explain the observations, assess the giant nuclei hypothesis, and point the way for future research. Some of these results were presented briefly in Ochs and Semonin (1977).

2. The model

The numerical simulations depicted the evolution of the droplet spectra in a rising parcel of air from an initial population of CCN and included the effects of condensation (or evaporation), coalescence and breakup. The ascent rate was prescribed and there was no entrainment or mixing with the parcel environment. In addition, the sedimentation of large drops into or out of the parcel was not considered. The model and numerical techniques employed were completely described in Ochs and Yao (1978) and Ochs (1978) and only a brief description of the important aspects of the model is presented here.

A small parcel of air was lifted at a chosen rate as the computation proceeded. During the adiabatic ascent several primary variables were computed as functions of time or altitude. Changes in water vapor mixing ratio, temperature and pressure were related to the condensation rate and updraft speed. In addition, the drop number concentration, average CCN mass per drop, and two moments of the drop concentration

0021-8952/79/091118-12$07.00

were retained within each Eulerian mass category. Changes in these variables resulted from condensational growth, stochastic collection and breakup.

As saturation was approached and exceeded in the rising parcel, condensation on the CCN occurred. The droplets grew in an Eulerian framework in which the mass doubles every second category. The droplet mass of category J was given by

$$x(J)=X_0 \exp[(J-1)/J_0)], \quad (1)$$

where J_0 is 2/ln2. Eq. (1) was only used to specify the mass at the center of each category. A linear mass coordinate was chosen within each category such that there was no discontinuity in drop mass at category end points and the ratio of adjacent category slopes was constant (Ochs and Yao, 1978).

An adaptation of Egan and Mahoney's (1972) numerical technique was used for the condensation, coalescence and breakup calculations (Ochs and Yao, 1978). This scheme had some important advantages when applied to this problem. First, the transport scheme employed strongly reduced numerical spreading of the droplet spectrum which would lead to premature development of large drops. Second, when used in conjunction with the piecewise linear mass coordinate previously discussed, the mass of the liquid water and CCN material was conserved to within computer truncation error (Ochs and Yao, 1978).

Objectively chosen variable time steps were used in all aspects of these computations. Short condensation and long collection time steps were used during the droplet activation stage since droplets moved rapidly through categories but were not large enough for many collections. Later, the drops grew very slowly by condensation allowing the long time step method of Clark (1973) to be used. When collection processes began to dominate the changes in the distribution shape, shorter collection time steps were adopted to preserve accuracy.

The equation for the condensational growth of droplets was given by Fukuta and Walters (1970). The equation was used under the assumption that the droplets were in thermal equilibrium with their environment. In addition, the density, osmotic coefficient and surface tension of the solution droplets were computed as functions of the mass ratio of solute to water. The temperature dependence of surface tension was also included.

The collection process was treated stochastically. The kernel employed was derived from the linear collision efficiencies, Y_c given by Jonas (1972), Klett and Davis (1973), Shafrir and Gal-Chen (1971) and Beard and Grover (1974). The terminal velocities were computed as functions of height by use of the methods of Beard (1976, 1977).

Two schemes for large-drop breakup were used simultaneously in the model. The first was that developed by Srivastava (1971) which treats the aerodynamic disintegration of large drops. Brazier-Smith *et al.* (1972, 1973) developed the second scheme in which drops undergoing off-center collisions, separate and produce satellites if the rotational energy generated by the collision exceeds the binding energy due to surface tension. Both of these methods were tested by Young (1975) who stated that the second scheme (collisional breakup) is more important than the first in determining the final drop distribution shape.

In this model the parcel was assumed to represent a rising volume in the center of a developing cumulus cloud. The crucial assumption was that the sedimentation of larger drops out of the parcel was not significant and that the drops that do fall out were replaced by similar drops from above. Most certainly, a proper treatment of sedimentation would affect the results. However, in cases where two precipitation distributions develop in the parcel with almost identical shapes and time histories, then one would expect that both cases would also develop similarly to each other if sedimentation effects were included. When the parcel calculations predict different developments, assessments become difficult. It was not the purpose of these calculations to predict the actual height at which a first radar echo develops, but to investigate the relative effects of changes in CCN concentration or composition on the initial development of precipitation.

3. Model initialization

The smaller size CCN in the initialized distribution were measured in the St. Louis area by other METROMEX participants (Fitzgerald and Spyers-Duran, 1973; Braham, 1974). Samples of air gathered during aircraft flights were analyzed in a diffusion cloud chamber immediately upon landing. Sedimentation of the larger particles and the inability to use very low supersaturations precluded the use of this technique for the measurement of giant CCN. The spectra measured are presented in the form

$$N=CS^k, \quad (2)$$

where N is the total number of CCN activated at a supersaturation S, and C and k are constants. The values of C and k were evaluated by varying S between 0.17 and 1.0% and applying a best-fit analysis to the data.

Since there were no data for giant CCN in the St. Louis urban area, an approximation to the tail of the CCN distribution was made. As a starting point, the distribution of Eq. (2) was extended until it intersected the total aerosol distribution given by $4\times10^{-12}\ r^{-3}$ particles cm^{-3} $(\ln r)^{-1}$, where r is the dry radius of the particle. The total aerosol curve was used for the CCN distribution beyond the intersection. The exponent of r was changed to -6.5 for particles $>40\ \mu$m radius as suggested by Noll and Pilat, (1971), and all distributions where truncated at a dry CCN radius of

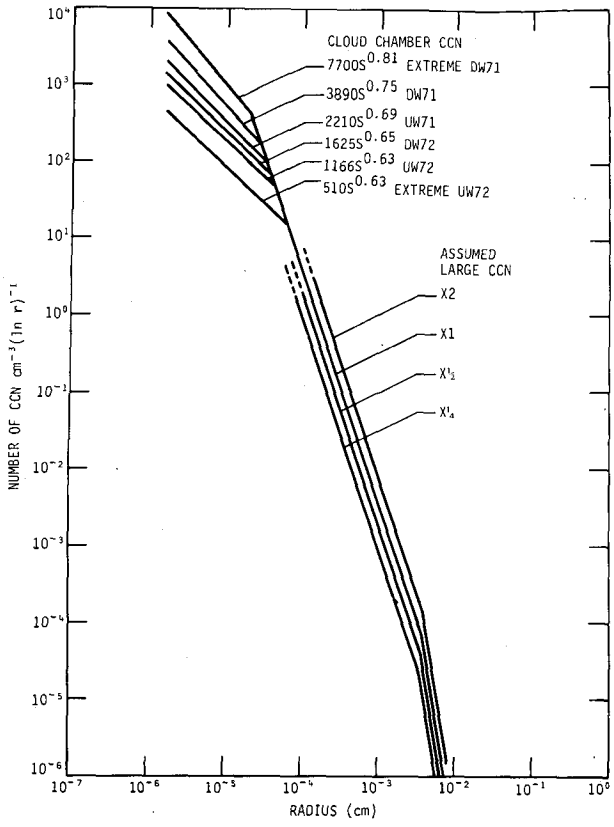

FIG. 1. Initial dry CCN radius (any of the observed cloud chamber CCN could be paired with one of the four assumed CCN distribution tails).

80 μm. Test calculations showed that the results are insensitive to this truncation value since there are too few nuclei of greater size to affect the processes considered. All of the particles in the entire CCN distribution were assumed to be composed of ammonium sulfate. This hybrid distribution formed the reference against which various changes in concentration, chemical composition and solubility were assessed.

The total aerosol portion of the CCN distribution was converted to saturated solution particles which provided the initial droplet concentrations in each category. The initialization of the segment of the distribution governed by Eq. (2) was slightly more complicated. Eq. (2) was used differentially in conjunction with the growth equation to determine the number density distribution in terms of the nuclei mass. The growth equation determined the activation supersaturation as a function of solution droplet physical properties. The nuclei material was then assumed to be in a saturated solution and the number density distribution was evaluated for the categories determined by Eq. (1).

To facilitate an accurate match to the data represented by Eq. (1), the CCN smaller than the point at which the cloud chamber data intersects the total aerosol curve were always assumed to be composed of soluble material of a single compound. Fitzgerald (1974) investigated the effects of populations of CCN with varying properties and found the resulting cloud droplet spectrum insensitive to these changes in the chemical makeup and partial solubilities of the CCN aerosol.

The initial temperature and pressure for all computations was 16.7°C and 886 mb. The parcel relative humidity was 83% and the mixing ratio was ~11.2 g kg^{-1}. These initial conditions produced saturation at ~850 mb and 13.1°C which were typical conditions for summer cloud bases in St. Louis.

The primary results are presented as plots of radar reflectivity versus simulated time. Radar reflectivity was chosen because METROMEX observations were often presented in terms of reflectivity and because it is a sensitive indicator of the presence of precipitation sized drops. The results could be given as functions of altitude; however, without sedimentation effects correct predictions of reflectivity heights are not possible. The importance of the results was evaluated by comparing computations. In order to indicate where drop sedimentation effects might be important, predicted distributions are presented for drops >100 μm radius.

4. Effects of variations in CCN concentrations

Fig. 1 presents the initial CCN distributions derived, in part, from the observations of Braham (1974) near St. Louis. The designation UW71 stands for the mean "upwind 1971" distribution and DW72 the mean "downwind 1972" distribution, etc. The extreme values shown were taken from scatter diagrams of all collected data. The CCN distribution labeled "extreme DW71" contained the greatest number concentration that was measured during the two summers, and similarly, the distribution labeled "extreme UW72" represents the least number concentration.

The total aerosol distribution used for CCN of

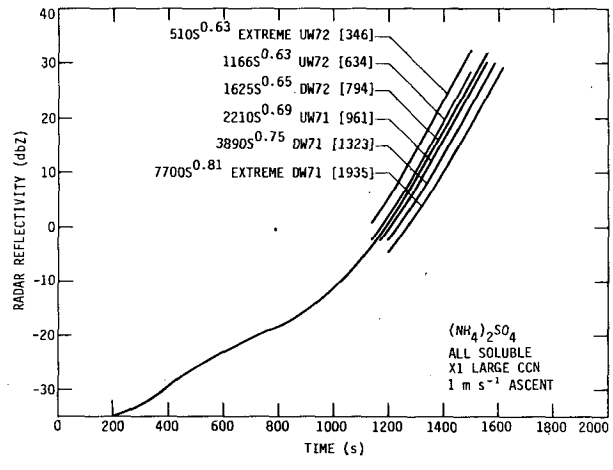

FIG. 2. Computed radar reflectivity factor for constant ascents and various cloud chamber CCN distributions.

$\gtrsim$0.5 μm radius is labeled $\times 1$ in Fig. 1. Those distributions labeled $\times 2$, $\times \frac{1}{2}$ and $\times \frac{1}{4}$ are the $\times 1$ distribution multiplied by 2, $\frac{1}{2}$ and $\frac{1}{4}$, respectively.

Fig. 2 depicts the model results of the calculated radar reflectivity factor obtained for a constant ascent rate of 1.0 m s^{-1}, and is plotted as a function of time for the six cloud chamber distributions with the $\times 1$ CCN distribution tail (the complete plot is given in only one case). For these cases all of the CCN were assumed to be completely soluble ammonium sulfate particles. Square brackets delineate the number of cloud droplets activated in each case. The most striking aspect of Fig. 2 is that in spite of the wide range in the number of activated cloud droplets (a difference of a factor of 5.6) all six parcels achieved a reflectivity of 20 dBZ within 150 s of each other.

This result was attributed to two nearly compensating effects. The downwind cases had higher cloud droplet concentrations and thus smaller mean sizes. Efficiencies for a small precipitation drop collecting the mean size cloud droplet were lower in the downwind cases but there were increased opportunities for collisions. The result was only a slight stabilization of the drop distribution for increased cloud droplet concentrations.

Evaluation of large-drop sedimentation effects on the results of Fig. 2 was difficult. However, we started with the premise that if two large-drop distributions evolved similarly and arrived at a detectable threshold radar reflectivity in about the same time then the same initial CCN distributions would produce similar results in a model that included sedimentation. The sedimentation model would not predict the same heights or times for first echoes as predicted by the parcel model but the two cases would still be similar since sedimentation would act equally on both.

Fig. 3 shows the distributions of drops $\gtrsim$0.1 mm radius from the extreme UW72 and DW71 cases presented in Fig. 2. Straight-line segments were used to connect the calculated data points. The computed reflectivities for the distributions shown differed by

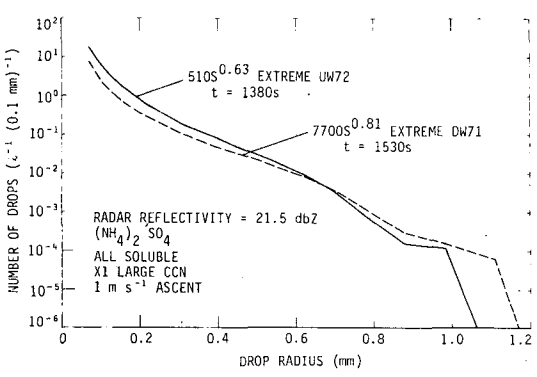

FIG. 3. Computed precipitation distributions at constant radar reflectivity for two simulations from Fig. 2.

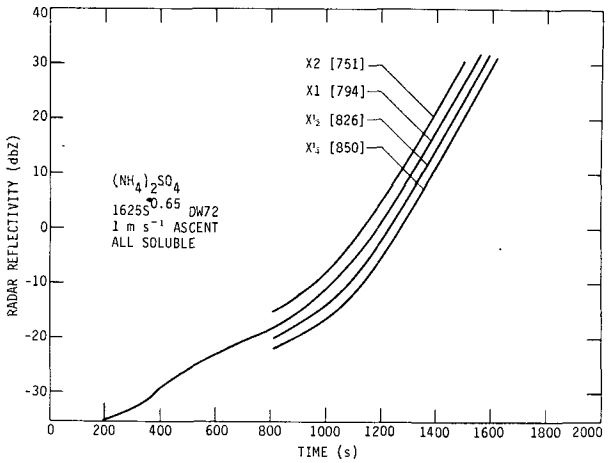

FIG. 4. Computed radar reflectivity factor for constant ascents and various CCN distribution tails.

only 0.014%. As can be seen, there was a slight tendency for the extreme DW71 CCN distribution to produce more of the largest drops at equivalent radar reflectivities. A factor affecting this result was the lower supersaturation in the cases with more activated drops. Thus, condensation on drops > 100 μm radius was reduced. Also in these cases there was more time for collisions to spread the distribution to larger sizes. Greater numbers of the largest drops would collect more intermediate drops (100–600 μm radius).

Analysis of the other cases in Fig. 2 showed that the large-drop distributions would lie between the extremes shown in Fig. 3. The analysis also indicated that all of the distributions evolved with very similar shapes. Since the time difference required to achieve equivalent radar reflectivities for the average upwind and downwind cases in the same year was so slight ($\lesssim$30 s), we conclude that first echoes would not be far apart in a sedimentation model.

Fig. 4 presents results obtained by varying the total aerosol portion of the CCN distribution with the DW72 cloud chamber distribution. With the constant 1.0 m s^{-1} ascent, a factor of 8 difference in the larger CCN concentration resulted in a 115 s difference in the time to achieve a radar reflectivity of 20 dBZ. Analysis of the drop distributions predicted in these cases showed that they all evolved similarly to the $\times \frac{1}{4}$ case which produced a slightly longer tail at 20 dBZ. The primary cause for the retarded reflectivities in this case was probably the fewer numbers of large droplets at cloud base which accreted cloud droplets at a lower rate. The longer times required to achieve 20 dBZ allowed the $\times \frac{1}{4}$ case large drop tail to spread to slightly larger sizes. From these cases we concluded that increasing the concentration of the largest CCN particles by factors of 2 slightly destabilized the droplet spectrum.

An additional series of computations was designed to

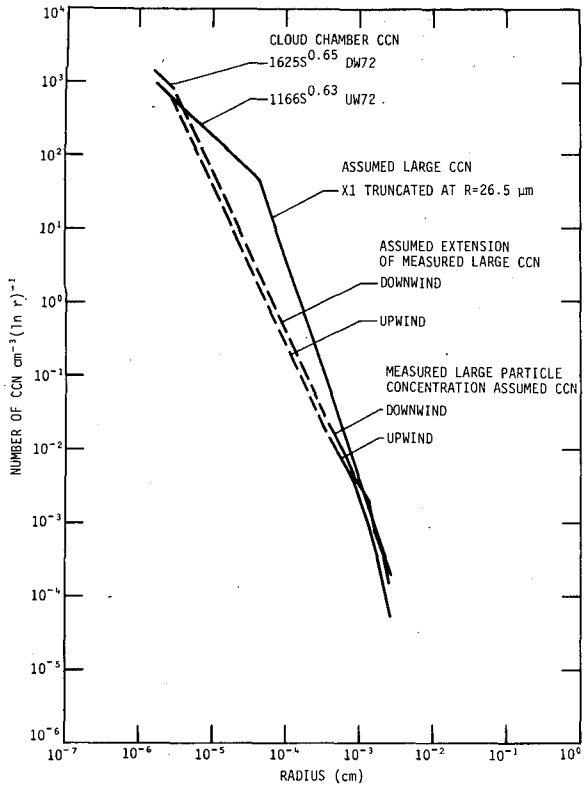

FIG. 5. Initial CCN distributions including measured ultragiant particle concentrations.

assess the effect of large-particle concentrations on the spectrum evolution. Johnson (1976) presented average distributions upwind and downwind of St. Louis for sizes between 5 and 55 μm diameter. These observations indicated that the average downwind total ultragiant particle volume was 1.8 times that of the average upwind volume. A summary of the 18 cases reported by Johnson indicates a maximum ratio of downwind to upwind particle volume of 4.4 and a minimum of 1.15.

Fig. 5 shows the initial distributions for this series of computations. Johnson's (1976) measured particles were assumed to be CCN and the data were extrapolated to smaller sizes until the UW72 and DW72 average data were intercepted. In addition, to the upwind and downwind combinations the UW72 distribution was combined with Johnson's downwind data. The UW72 cloud chamber CCN spectrum with the $\times 1$ tail truncated at 26.5 μm radius was included for comparison. The calculated radar reflectivities shown in Fig. 6 exhibit very little difference between any of these cases. This series of computations indicated the relative unimportance to eventual precipitation formation of factors of 5 and greater in CCN concentrations in the intermediate range of 0.2 to 2 μm radius. More importantly, note that the two cases which combine average data for upwind and downwind CCN arrived at 20 dBZ in almost identical times. The computed drop spectra showed that these cases evolved with very similar shapes as depicted in Fig. 7. Thus, we concluded that a sedimentation model with a complete microphysical treatment would also lead to the result that the increased drop spectrum stability caused by increased nuclei concentrations in downwind and urban air is essentially offset by the increase in larger particles. Dytch and Johnson (1977) used a model that allowed drop sedimentation and included condensation and continuous collection with a single cloud droplet category to investigate average upwind and downwind cases. They predicted a slightly lower echo base in downwind clouds; however, Johnson (1979) indicates that subsequent improved studies showed no upwind-downwind difference.

5. Effects of variations in CCN chemical composition

The effect of the CCN chemical properties on the development of precipitation was studied by comparing the evolution of drop distributions initiated with both sodium chloride and ammonium sulfate. The NaCl computations were initialized at a relative humidity of 80% as opposed to 83% for the $(NH_4)_2SO_4$.

The DW72 cloud chamber CCN spectrum with the $\times 1$ tail was used and the method of initialization remained the same as in the previous cases. The tail of the distributions was identical for both chemical compositions since the number concentration of particles was specified by the total aerosol distribution. However, in the region where the diffusion cloud chamber data were used to specify the CCN distribution, the initial number concentrations were slightly different although the same data given by Eq. (2) were used. To activate the same number of particles at a given supersaturation there were fewer NaCl than $(NH_4)_2SO_4$ particles in a given size interval since NaCl is more hygroscopic than $(NH_4)_2SO_4$. For the

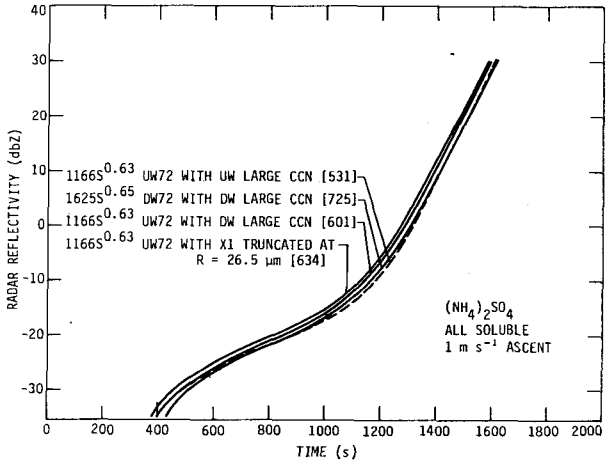

FIG. 6. Computed radar reflectivity factor for the CCN distributions in Fig. 5.

chosen distribution there were 16% more ammonium sulfate than sodium chloride particles per radius interval centered at 0.1 μm.

Fig. 8 shows the results of two computations in which the parcels were lifted at a constant 4 m s^{-1}. The numbers in square brackets indicate the number of activated drops in each case. The results showed that the sodium chloride distribution achieves a radar reflectivity of 20 dBZ at ~200 m lower than the ammonium sulfate case. Analysis of the predicted cloud droplet distributions confirms the findings of Fitzgerald (1974) who showed that the distributions are not sensitive to the chemical composition of the soluble material in the CCN. Therefore, with nearly identical cloud droplet distributions one would expect a similar evolution of radar reflectivity. A comparison of the evolving large drop distributions showed no tendency for one case to develop the largest drops faster than the other.

6. Effects of variations in CCN solubility

Several computations were performed with particles greater than a given size in the initial CCN distribution tail assumed to be composed of insoluble particles that contain a very small amount of soluble material. The insoluble particles were simulated with pure water drops that were not permitted to evaporate while the parcel is subsaturated. When the parcel achieved supersaturation, the water drops grew by condensation without solution effects. The introduction of pure water drops simulated the rapid dilution and subsequent growth of an insoluble particle with a vanishingly small amount of soluble material on its surface (Junge and McLaren, 1971). The collection of solution droplets by larger water drops did not influence condensational growth of the resulting drop since it contained a very dilute solution. A discontinuity in the droplet number density distribution was present at the onset of the computations. This condition arose because the ammonium sulfate particles were initialized

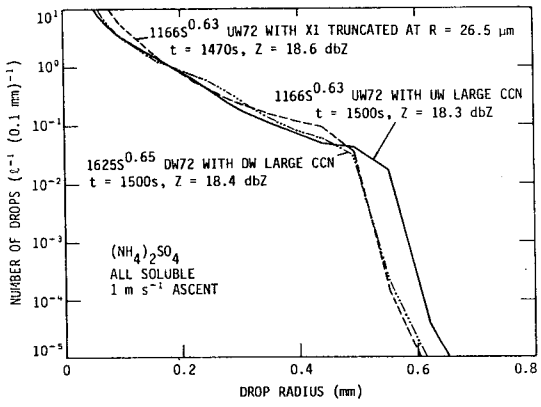

FIG. 7. Computed precipitation distributions at nearly constant radar reflectivity for three cases in Fig. 6.

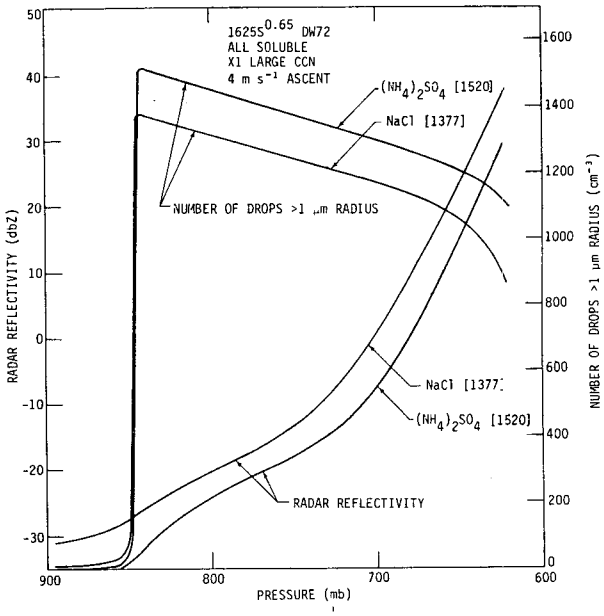

FIG. 8. Computed radar reflectivity factor and number of drops >1.0 μm radius for equivalent CCN distribution concentrations and different chemical compositions.

as small saturated solution droplets at 83% relative humidity, but the large water drops used to simulate dry insoluble CCN were already specified in the distribution.

Fig. 9 presents results obtained by varying the point at which the insoluble distribution begins. The DW72 CCN distribution with the ×1 large CCN tail and a 4.0 m s^{-1} ascent rate was employed. The computations showed that the solubility of particles in the range between ~15 and 50 μm radius can affect the evolution of radar reflectivity. The data presented in Fig. 9 also indicated the insensitivity of the number of activated cloud drops to the properties of the CCN in the distribution tail. Less than a 2% variation in the number of activated droplets was computed in the six cases.

Two effects contributed to the variations of calculated time to reach the various reflectivity levels depicted in Fig. 9. First, there was the reduced size of the initial drops that represented the insoluble particles. Second, the essentially pure water drops were not permitted to grow until saturation was achieved and then they grew very slowly in the slightly supersaturated parcel. On the other hand, droplets formed from pure ammonium sulfate CCN in the distribution tail lagged far behind their equilibrium radius and thus could condense significant amounts of water vapor both before and after saturation was reached.

In order to assess the relative importance of these two factors an additional computation was made. The number density distribution for the all-soluble $(NH_4)_2SO_4$ case shown on Fig. 9 was employed with pure water drops making up the spectrum beyond 1.5 μm radius. In this hypothetical case, the CCN were

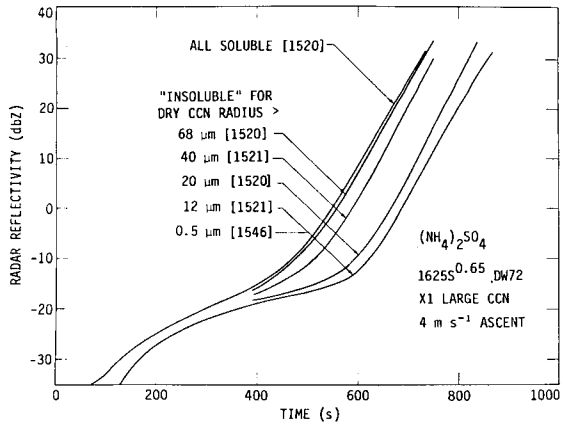

FIG. 9. Computed radar reflectivity factor for a CCN distribution in which particles greater than a chosen size were assumed to be insoluble with a very thin coating of soluble material.

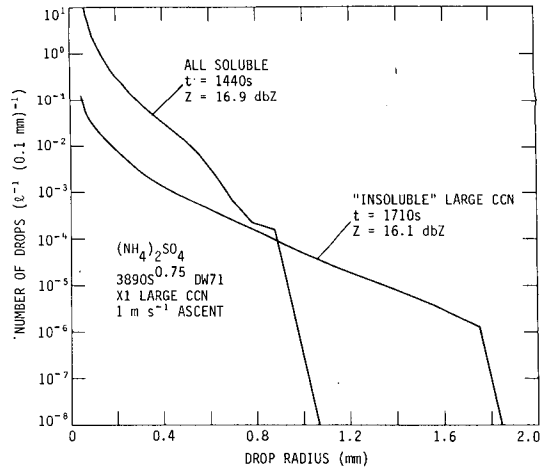

FIG. 11. Computed precipitation distributions at nearly constant radar reflectivities for two cases from Fig. 10.

artificially given the same initial increase in size that would occur if they had been composed of $(NH_4)_2SO_4$ and had deliquesced at 83% relative humidity, but they were not permitted the subsequent benefit in growth rate from the solute. The results indicated that the development of radar reflectivity was retarded by ~45 s from the all-soluble $(NH_4)_2SO_4$ CCN case. The corresponding case in which the insoluble CCN were initialized at their dry radius was delayed from the soluble case by 140 s. Therefore, both the initial size change for the pure ammonium sulfate CCN and the solution effects on condensational growth were significant in assessing the reasons for the delayed radar reflectivities in Fig. 9.

The DW71 distribution was chosen to illustrate the combined effects of solubility and number concentrations in the distribution tail. Fig. 10 shows the evolution of radar reflectivity for initial CCN containing pure ammonium sulfate and insoluble large CCN initialized as pure water drops beyond 5 μm radius with the $\times 1$ and $\times \frac{1}{2}$ distribution tails. The results showed a significantly greater dependence on extreme differences in solubility than on the factor of 2 changes in CCN concentrations in the distribution tail. Identical sets of calculations were performed for the other three average summer cloud chamber CCN distributions with the same results.

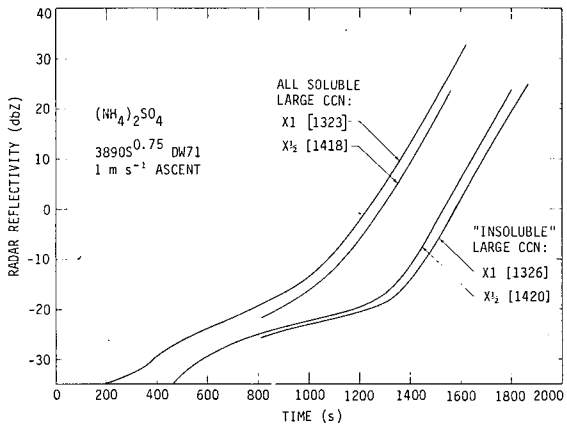

FIG. 10. Computed radar reflectivity for different CCN distribution tails and solubilities.

Since the number of droplets activated in the corresponding soluble and insoluble cases presented in Fig. 10 were almost identical, the supersaturation during the time that the radar echo developed was also nearly identical. However, as was discussed, there were significant differences in the ability of CCN > 5 μm radius to grow by condensation. Also initial size differences between soluble and insoluble cases resulting from the deliquescence of the soluble CCN contributed to the computed differences in the evolving radar reflectivity. Since the insoluble cases required longer time periods to achieve the same radar reflectivity as the all soluble cases, the distributions spread by collection to larger sizes. In fact, differences in the evolution of condensation and collection were large enough so that the drop distributions for the two $\times 1$ cases of Fig. 10 differed as shown in Fig. 11. From Fig. 11 we conclude that neglected sedimentation effects should be important since the insoluble cases had more time for sedimentation and developed larger drops which would fall faster. Although it was impossible to accurately quantify the outcome using our results, a sedimentation model would show a lowering of the echo base in the insoluble cases with respect to the all-soluble cases.

In order to more completely assess the effects of partial solubility on the evolution of precipitation, several computations were performed with the CCN mass in the distribution tail composed of soluble and insoluble fractions. The DW72 cloud chamber CCN distribution coupled with the $\times 1$ tail and a 1 m s^{-1} ascent rate was used. The insoluble fraction was assumed to have a density of 2.0 g cm^{-3} and, as in

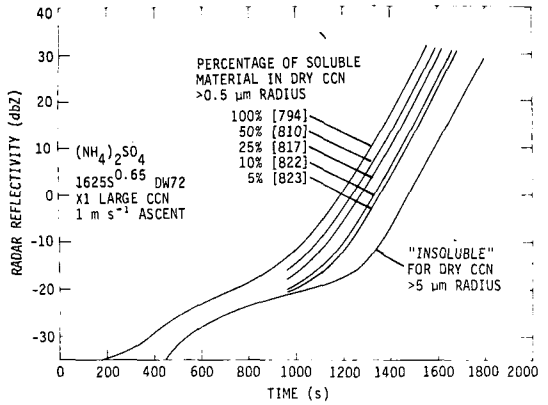

FIG. 12. Computed radar reflectivity factors for a CCN distribution in which the largest CCN were assumed to have constant partial solubilities ranging from 100% to 0%.

previous calculations, all masses were conserved to computer truncation error. The soluble portion of the CCN was assumed to be ammonium sulfate. When the droplets were initialized in the parcel the soluble fraction of the nuclei mass was assumed to be in a saturated solution that completely surrounded the insoluble portion of the CCN particle. In the cases presented in Fig. 12 all CCN $\gtrsim 0.5$ μm radius were assumed to have some insoluble material, and the corresponding case is presented in which CCN > 5 μm were almost entirely insoluble. The results indicate that over a wide range of partial solubilities radar reflectivity develops much faster than for the insoluble case.

In each case presented in Fig. 12, the initial concentration distributions of dry CCN sizes were identical. Thus, the variation in the temporal development of radar reflectivity depicted in Fig. 12 was attributed to essentially two interacting factors. First, the CCN with larger fractions of soluble material become larger solution droplets when they deliquesced at the onset of the calculation. Second, the droplets with smaller

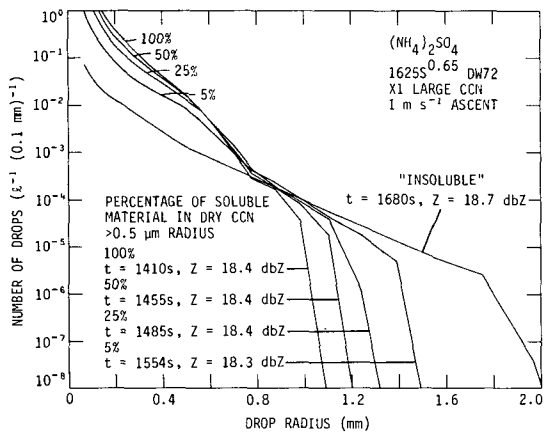

FIG. 13. Computed precipitation distributions at nearly constant radar reflectivity for the cases from Fig. 12.

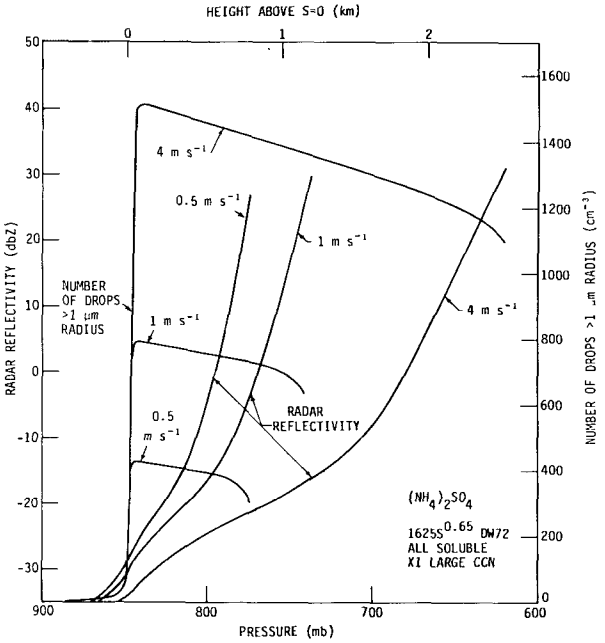

FIG. 14. Computed radar reflectivity factor and number of drops >1.0 μm radius for various constant ascent rates.

fractions of soluble material diluted faster as condensation proceeded thus reducing the subsequent condensation rate. The net effect was that CCN, with a small fraction of soluble material, started as smaller droplets and did not grow as large by condensation, which reduced growth by the collection process. These effects maximized in the insoluble case which required longer to achieve a reflectivity level so that growth by collection could overcome deficiencies in the initial sizes and subsequent condensational growth rates of the drops in the distribution tail. Fig. 13 clearly shows the results of these factors on the precipitation drop distributions. These distributions also show that a relatively small amount of soluble material in the initial CCN allowed the spectrum to develop more like the all-soluble case than the insoluble case.

7. Effects of variations in vertical speed

Model computations were made with three parcel ascent rates. The results depicted in Fig. 14 were obtained with the DW72 cloud chamber CCN distribution and the $\times 1$ tail. All CCN were assumed to be pure ammonium sulfate.

Fig. 14 shows that increased parcel ascent speeds resulted in larger concentrations of cloud droplets. The results depicted in Fig. 2 show that increased numbers of cloud drops in cases with identical CCN tails did not greatly retard the development of precipitation. With identical ascent speeds above the activation region, predictions nearly the same as those of Fig. 2 would result regardless of the cause of differing cloud droplet concentrations at cloud base. Therefore, the

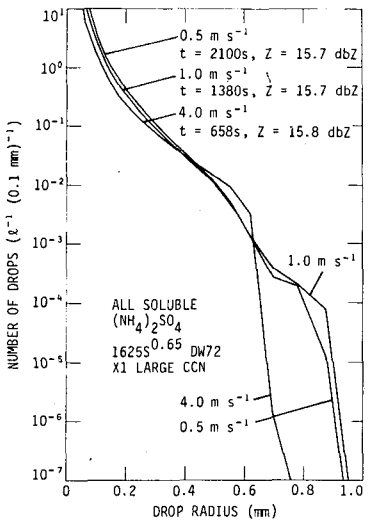

FIG. 15. Computed precipitation distributions at nearly constant radar reflectivities for the cases from Fig. 14.

cause of the increased elevation of equivalent radar reflectivities in the higher updraft cases in Fig. 14 was that they had less time at each level for collections to produce larger drops.

The 4.0 m s^{-1} case arrives at 15.7 dBZ in the shortest time (Fig. 15). The amount of water vapor condensed as the parcel moves between two levels was approximately equal to the difference in the water vapor necessary to saturate the parcel at the two levels. Most of this water condensed on the cloud drops which shared almost equally in the total condensate. A strong feedback in the governing equations adjusted the supersaturations such that this outcome was assured. As the 4.0 m s^{-1} parcel achieved higher elevations its more numerous cloud drops grew to larger sizes where collection efficiencies increase. Thus, accretion rates became large enough at the higher elevations to allow the 4.0 m s^{-1} case to achieve a given radar reflectivity in less total time than the other cases.

Fig. 15 shows the predicted drop distributions for the three cases of Fig. 14 at a radar reflectivity near 15.7 dBZ. The largest drops in the spectra were produced by coalescences between nearly equal sized drops in the next two smaller categories. Apparently, the 4.0 m s^{-1} case could not produce the same maximum sized drops as in the other two parcels because of the reduced time needed to achieve 15.7 dBZ. Since sedimentation acts longer in the slower moving parcels and the 4.0 m s^{-1} case had smaller maximum sized drops which are more effectively carried aloft by higher ascent speeds, a model containing sedimentation effects would be expected to increase the predicted differences in elevations of equivalent radar reflectivities.

Three calculations were made to investigate the effect of different updraft speeds above the region where activation occurs. A hypothetical cloud chamber CCN distribution of 1000 $S^{0.7}$ was coupled with the $\times 1$ large CCN distribution for these calculations. The ascent rate was held constant at 3.0 m s^{-1} until a liquid water content of 0.1 g m^{-3} was achieved with 939 cloud droplets in each parcel. Beyond this point the vertical speed of the parcels was increased at 1.0 and 2.0 m s^{-1} km^{-1}. The results are shown in Fig. 16. A radar reflectivity of 20 dBZ was achieved in 567 and 523 s beyond the 0.1 g m^{-3} point, as opposed to 621 s for the constant 3.0 m s^{-1} case.

An examination of the predicted precipitation distributions for these cases showed essentially identical distributions at equivalent radar reflectivities. Recalling that the drop distributions were identical at a liquid water content of 0.1 g m^{-3}, the parcels that attain a greater elevation at a given value of radar reflectivity should contain larger cloud drops. Since less water vapor was required to saturate the parcel at higher elevations, the excess was condensed. Most of the condensation occurred on the cloud drops which shared approximately equally in this excess water. For example, at 15 dBZ the parcel with a constant ascent rate contained cloud droplets with a mean size of 9.8 μm, while the parcel with the 2.0 m s^{-1} km^{-1} increasing ascent rate contained droplets with a 10.9 μm mean size. However, the constant updraft parcel required 90 s longer to achieve the 15 dBZ level. Thus, the constant updraft parcel had a longer time for collections to spread the spectrum to larger sizes, but it had slightly

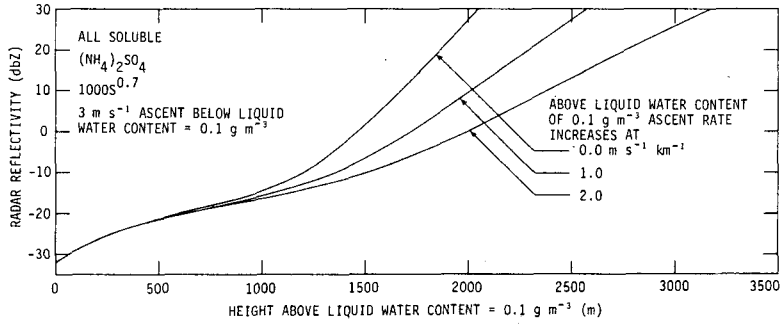

FIG. 16. Computed radar reflectivity factor for various lapse rates of parcel velocity above the point at which a liquid water content of 0.1 g m^{-3} is achieved.

smaller cloud droplets which would inhibit transfer of liquid water to the precipitation distribution. These compensating effects lead to an almost identical largest size drop at a given value of radar reflectivity for the cases presented in Fig. 16. The higher vertical velocities attained in the cases that developed detectable radar reflectivities at greater elevations would cause these parcels to carry precipitation aloft more effectively than the lower, slower moving parcels. For example, at the 20 dBZ level the 0.0, 1.0 and 2.0 m s^{-1} km^{-1} cases achieved vertical speeds of 3.0, 5.3 and 8.5 m s^{-1}, respectively. This is important since if sedimentation effects were considered in the model, they would lead to further separation of the vertical locations of detectable radar reflectivities.

8. Discussion of observations, model results and further speculation

Fitzgerald and Spyers-Duran (1973) and Braham (1974) found increased concentrations of both cloud chamber CCN and cloud droplets in samples gathered downwind of the St. Louis urban-industrial complex compared with upwind samples. These observations agree qualitatively with our model predictions.

Radar observations (Braham and Dungey, 1978; Changnon, 1978) and cloud-base height measurements (Semonin and Changnon, 1974) showed that the bases of urban first echoes are closer to the cloud bases than in similar rural clouds. The urban first echoes were 300–500 m lower and the cloud bases 300–600 m higher than their rural counterparts. Other data support elevated urban cloud bases. The average pre-rain soundings of Ackerman and Appleman (1974) taken in the center of the city at the St. Louis Arch and 22 km east indicated an $\sim$600 m greater elevation for the convective condensation level at the Arch. Further support is derived from the numerous surface and aircraft data which indicated that the boundary layer was warmer and drier in the urban area (see, e.g., Sisterson, 1975).

The increased cloud droplet concentrations and the lesser distance between cloud base and the first echo base found in urban clouds led Braham (1974) and Semonin (1974) to hypothesize the presence of increased concentrations of giant CCN to explain the apparent increase in efficiency with which urban clouds produced first echoes. A measurement project was initiated and Johnson (1976) reported increased concentrations of large particles in urban air compared with the rural surroundings. He indicated that particles in both urban and rural samples appeared to be insoluble with a thin coating of soluble material (personal communication). Ochs and Gatz (1979) have measured the average solubility of all particles > 5 μm diameter during a two-week period in the summer of 1977 in Champaign, as an indication of the properties of such large particles. The average percentage of soluble material found by Ochs and Gatz was 30%.

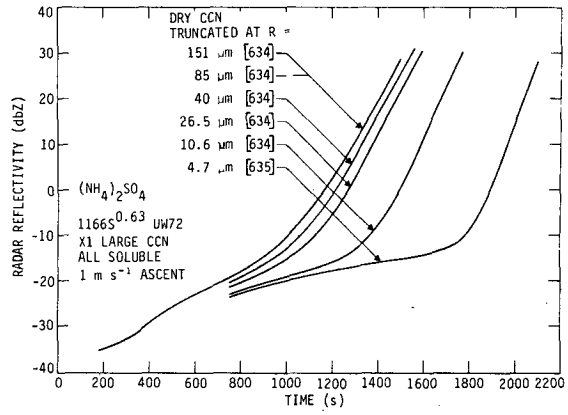

FIG. 17. Computed radar reflectivity for parcels with CCN distributions truncated at various dry CCN radii.

The model results indicated that variations in CCN concentrations in the small, large and giant size ranges did not explain the METROMEX observations of urban-rural first echo differences. Variations in CCN concentrations were made which equalled or exceeded the maximum spread in the field observations.

A point of interest is that the model computations did not indicate that giant nuclei (> 1.0 μm radius) were unimportant to the precipitation process. Figure 17 shows the results of systematically eliminating CCN whose size exceeded given values. For the distribution of soluble CCN employed in these computations, particles > 40 μm in radius had little effect on the time for development of a given radar reflectivity, primarily because their initial concentrations were too low to be effective. On the other hand, if CCN > 5 or 10 μm were eliminated, the development of precipitation was retarded significantly. Thus, CCN between 5 and 40 μm radius are important to precipitation formation in this case, and the model only suggests that the observed variations in the concentration of CCN > 5 μm radius do not appear to account for the first echo observations of urban and rural clouds.

Effects of variations in the chemical or physical makeup of CCN on precipitation evolution were also studied. The results showed that differences similar to those between sodium chloride and ammonium sulfate were insufficient to explain the field observations. In addition, the model results showed that highly hygroscopic CCN would probably lead to a reduction in the number of activated cloud droplets. Since this result was contrary to the observed increases in cloud-base droplet concentrations in urban clouds, the observations cannot be explained by the presence of hygroscopic CCN.

The modeling results, as well as the available observational evidence, suggested that the partial solubility of the largest CCN was probably not the explanation of the field observations. Moreover, there is some quantitative observational evidence that the required

large difference in urban-rural giant CCN partial solubility does not exist (D. B. Johnson, personal communication).

Results of this modeling research suggested that dynamic effects could easily account for the cloud echo observations. These results coupled with observational evidence can lead to a hypothesis for explaining first echo observations. There were increases in average cloud base heights above the St. Louis–East St. Louis area. Urban and rural soundings showed a drier and warmer subcloud layer over St. Louis than over rural areas. These data also showed that the average pre-rain soundings were very similar above the cloud base predicted by the convective condensation level over St. Louis. Since new convective clouds over St. Louis had higher cloud bases, they would have developed along moist adiabats with lower equivalent potential temperatures than similar rural clouds. The lower equivalent potential temperatures in the St. Louis clouds would have resulted in less buoyancy and thus reduced updraft speeds and slower development in the similar above cloud base environments. This reasoning suggested that these dynamic effects in clouds developing over St. Louis could explain the observations.

Future research should test the hypothesis presented here for explaining the observed cloud base to first echo distances. A time-dependent cloud model which incorporates a detailed simulation of cloud microphysics could be used for this purpose. Current models with Eulerian grid spacings may be sufficient to assess the observed difference between average cloud base and first echoes over the city and rural areas. These differences of $\sim$1000 m should be detectable in models with grid spacings of $\sim$100 m providing that sufficiently accurate numerical techniques are employed. Ackerman and Appleman's (1974) pre-rain soundings could be used. Another aspect of this topic worth pursuing would be to subdivide Braham and Dungey's (1978) city area to determine if there are any significant differences between first echoes occurring over the St. Louis–East St. Louis area where Semonin and Changnon (1974) report higher cloud bases and the Alton-Wood River area to the North of the St. Louis Arch where cloud bases were more like those in rural areas.

Acknowledgments. The authors would like to acknowledge Dr. Kenneth V. Beard for his helpful comments during the course of the research and for his comments on the final manuscript. Julie K. Lewis and Rebecca A. Runge typed the manuscript and John Brother drafted the figures.

This research was performed under Grant ENV73-07782 as part of the research on METROMEX, sponsored by the Weather Modification Program, Research Applications Directorate, National Science Foundation, and the Department of Energy under Contract EY-76-S-02-1199. The computations were performed on the National Center for Atmospheric Research CDC 7600 Computer.

REFERENCES

Ackerman, B., and H. Appleman, 1974: Boundary-layer program. Interim Report of METROMEX Studies: 1971–1973, F. A. Huff, Ed., NSF Report, Grant GI-38317, 121–142.

Beard, K. V., and S. N. Grover, 1974: Numerical collision efficiencies of small raindrops colliding with micron size particles. *J. Atmos. Sci.*, **31**, 543–550.

——, 1976: Terminal velocity and shape of cloud and precipitation drops aloft. *J. Atmos. Sci.*, **33**, 851–864.

——, 1977: Terminal velocity adjustment for cloud and precipitation drops aloft. *J. Atmos. Sci.*, **34**, 1293–1298.

Braham, R. R., 1974: Cloud physics of urban weather modification: A preliminary report. *Bull. Amer. Meteor. Soc.*, **55**, 100–105.

——, and M. J. Dungey, 1978: A study of urban effects on radar first echoes. *J. Appl. Meteor.*, **17**, 644–654.

Brazier-Smith, P. R., S. G. Jennings and J. Latham, 1972: The interaction of falling water drops: coalescence. *Proc. Royal Soc. London*, **A326**, 393–408.

——, —— and ——, 1973: Raindrop interactions and rainfall rates within clouds. *Quart. J. Roy. Meteor. Soc.*, **99**, 260–272.

Changnon, S. A., 1978: Vertical characteristics and behavior of radar echoes. *Summary of METROMEX*, Vol. 2, *Causes of Precipitation Anomalies*, B. Ackerman *et al.*, Illinois State Water Survey, Bull. No. 63, Urbana, 274–279.

——, F. A. Huff, and R. G. Semonin, 1971: METROMEX: An investigation of inadvertent weather modification. *Bull. Amer. Meteor. Soc.*, **52**, 958–967.

Clark, T. L., 1973: Numerical modeling of the dynamics and microphysics of warm cumulus convection. *J. Atmos. Sci.*, **30**, 857–877.

Dytch, H. E., and D. B. Johnson, 1977: Urban influences on warm cloud microstructure. *Preprints Sixth Conf. Planned and Inadvertent Weather Modification*, Champaign, Amer. Meteor. Soc., 37–40.

Egan, B. A., and J. R. Mahoney, 1972: Numerical modeling of advection and diffusion of urban area source pollutants. *J. Appl. Meteor.*, **11**, 312–322.

Fitzgerald, J. W., and P. A. Spyers-Duran, 1973: Changes in cloud nucleus concentration and cloud droplet size distribution associated with pollution from St. Louis. *J. Appl. Meteor.*, **12**, 511–516.

——, 1974: Effect of aerosol composition on cloud droplet size distribution: A numerical study. *J. Atmos. Sci.*, **31**, 1358–1367.

Fukuta, N., and L. A. Walters, 1970: Kinetics of hydrometeor growth from a vapor-spherical model. *J. Atmos. Sci.*, **27**, 1160–1172.

Huff, F. A., and S. A. Changnon, 1972: Climatological assessment of urban effects on precipitation at St. Louis. *J. Appl. Meteor.*, **11**, 823–842.

Johnson, D. B., 1976: Ultragiant urban aerosol particles. *Science*, **194**, 941–942.

——, 1979: The role of coalescence nuclei in warm rain initiation. Ph.D. thesis, The University of Chicago, 119 pp.

Jonas, P. R., 1972: The collision efficiency of small drops. *Quart. J. Roy. Meteor. Soc.*, **98**, 681–683.

Junge, C., and E. McLaren, 1971: Relationship of cloud nuclei spectra to aerosol size distribution and composition. *J. Atmos-Sci.*, **28**, 382–390.

Klett, J. D., and M. H. Davis, 1973: Theoretical collision efficiencies of small cloud droplets at small Reynolds number. *J. Atmos. Sci.*, **30**, 107–117.

Noll, K. E., and M. J. Pilat, 1971: Size distribution of atmospheric giant particles. *Atmos. Environ.*, **5**, 527–540.

Ochs, H. T., 1978: Moment conserving techniques for microphysical computations, Part II: Model testing and results. *J. Atmos. Sci.*, **35**, 1959–1973.

——, and R. G. Semonin, 1977: The sensitivity of cloud microphysics to an urban environment. *Preprints Sixth Conf. Planned and Inadvertent Weather Modification*, Champaign, Amer. Meteor. Soc., 41–44.

——, and C. S. Yao, 1978: Moment conserving techniques for microphysical computations, Part I: Numerical techniques. *J. Atmos. Sci.*, **35**, 1947–1958.

——, and D. F. Gatz, 1979: Water solubility of atmospheric aerosols. Submitted to *Atmos. Environ.*

Semonin, R. G., 1974: Urban-induced weather modification. *Earth Environment and Resources Conf. Digest of Tech. Papers*, Vol. 1, IEEE Cat. No. 74CH0876-3EQC, New York, 40–41.

——, and S. A. Changnon, 1974: METROMEX: Summary of 1971–1972 results. *Bull. Amer. Meteor. Soc.*, **55**, 95–99.

Shafrir, U., and T. Gal-Chen, 1971: A numerical study of collision efficiencies and coalescence parameters for droplet pairs with radii up to 300 microns. *J. Atmos. Sci.*, **28**, 741–751.

Sisterson, D. L., 1975: Studies on the urban moisture budget. Rep. AS114, Dept. Atmos. Sci., College of Engineering, University of Wyoming, 141 pp.

Srivastava, R. C., 1971: Size distribution of raindrops generated by their breakup and coalescence. *J. Atmos. Sci.*, **28**, 410–415.

Young, K. C., 1975: The evolution of drop spectra due to condensation, coalescence and breakup. *J. Atmos. Sci.*, **32**, 965–973.